THE JOURNAL OF PHYSICAL CHEMISTRY A

 VOLUME 109, NUMBER 12, MARCH 31, 2005

ARTICLES

Wavelength-Dependent Stereodifferentiation in the Fluorescence Quenching of Asymmetric Naphthalene-Based Dyads by Amines

Sergio Abad,[†] Uwe Pischel,*[,‡] and Miguel A. Miranda*[,†]

Instituto de Tecnología Química, Universidad Politécnica de Valencia, Av. de los Naranjos s/n, E-46022 Valencia, Spain, and REQUIMTE/Departamento de Química, Faculdade de Ciências, Universidade do Porto, Rua Campo Alegre, 4169-007 Porto, Portugal

Received: May 10, 2004; In Final Form: January 27, 2005

In the present contribution, wavelength has been used as a tunable parameter to achieve selective control of the photophysics of two novel asymmetric bichromophoric dyads composed of naphthalene units, i.e., 6-methoxynaphthalene (NPX) and 1-methylnaphthalene (NAP) derivatives, with different electronic properties, connected by an amide spacer [(*S*,*S*) and (*S*,*R*)-NPX-NAP]. As model systems, relevant monochromophoric compounds (NPX-M and NAP-M) have also been investigated. While upon excitation at 325 nm the light energy remained in the NPX moiety, at 290 nm an efficient singlet−singlet energy transfer (Φ_{SSET} of about 97%) from the NAP unit to the NPX chromophore dominated. A remarkable stereodifferentiation was observed in the excited-state quenching by triethylamine via exciplex formation. The results demonstrate that it is possible to control configuration-dependent interactions in the excited state by wavelength tuning. This can be rationalized through intramolecular interactions of π systems leading to modulation of the redox properties.

Introduction

Wavelength has been used as a tunable parameter to gain selective control of photophysical and photochemical processes.[1−5] Wavelength-dependent photophysics and/or photochemistry has been clearly demonstrated in a number of examples.[3,6−10] The case of bi- (or poly-) chromophoric compounds is of particular interest, in connection with the possibility of light absorption at a specific chromophore, keeping it localized until finishing the photochemical reaction. This is the origin of so-called "orthogonal" photochemistry.[4,5]

Recently, asymmetric photochemistry has attracted considerable attention.[11,12] Its control can be achieved by variation of several parameters, such as temperature, pressure, or solvent; in the solid phase the chiral information can also be provided by a rigid environment.[11,12] In this context, it would be highly desirable to control configuration- or conformation-dependent interactions in the excited state by adequate selection of the excitation wavelength. To our knowledge, this possibility has been explored only for few examples,[6−8,10,13] despite its potential interest.

Several factors are known to control the kinetics of excited-state interactions via electron transfer, exciplex formation, hydrogen transfer, or energy transfer.[14−17] Extensive investigations have been devoted to steric[18−21] or stereoelectronic effects,[21−23] spin multiplicity,[21,24] and electronic effects.[21,25−28] In our recent research we became interested in the question of whether chirality might influence the quenching of excited states. Our conceptual approach includes the design of diastereomeric dyads, among them benzophenone/hydrogen donor and naph-

* To whom correspondence should be addressed. M.A.M.: tel, +34 96 3877 807; fax, +34 96 3877 809, e-mail, mmiranda@qim.upv.es. U.P.: tel, +351 22 608 2885; fax, +351 22 608 2959; e-mail, upischel@fc.up.pt.
[†] Instituto de Tecnología Química, Universidad Politécnica de Valencia.
[‡] REQUIMTE/Departamento de Química, Faculdade de Ciências, Universidade do Porto.

10.1021/jp047996a CCC: $30.25
Published on Web 03/04/2005

CHART 1

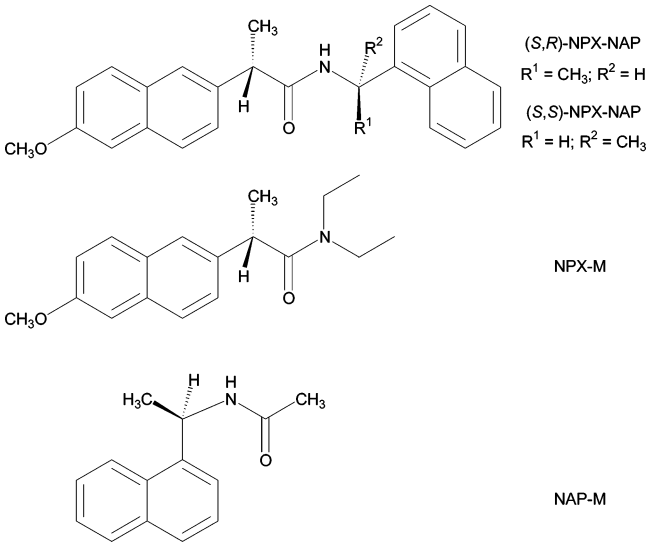

thalene/electron donor combinations.[29−36] For the majority of the investigated dyads, pronounced diastereodifferentiation has been observed, albeit the size of the effect is dependent on the conformational and thermodynamic requirements of each system.

In the present contribution, we report on the photophysics of two novel asymmetric and bichromophoric dyads (NPX-NAP) composed of naphthalene units with different electronic properties, connected by an amide spacer (cf. Chart 1). As model systems, the relevant monochromophoric compounds NPX-M and NAP-M (cf. Chart 1) have been investigated. The significantly different absorption spectra of both naphthalene units allow for selective or at least preferential excitation of one or the other chromophore in the dyads. A remarkable influence of the chiral information on *intermolecular* exciplex-induced quenching by triethylamine[37−44] has been observed.

Experimental Section

Materials. All materials for the synthesis of the dyads and model compounds were purchased from Aldrich and used without further purification. *n*-Hexane as the solvent for absorption and fluorescence measurements was of spectroscopic quality from Merck. Silica gel (230−400 mesh) from Scharlau was used for column chromatography. Ethyl acetate and *n*-hexane from Scharlau were the eluting solvents for flash chromatography. Triethylamine (99%) from Aldrich was used as received.

Spectroscopic Measurements. UV/vis absorption measurements were performed on a Shimadzu UV-2101PC spectrometer. Fluorescence emission and excitation spectra were recorded on a Photon Technology International (PTI) LPS-220B fluorimeter. All spectra, except for relative measurements of fluorescence quenching, are corrected for the instrument response. Lifetimes were measured with a lifetime spectrometer (TimeMaster fluorescence lifetime spectrometer TM-2/2003) from PTI by means of the stroboscopic technique, which is a variation of the boxcar technique. As the excitation source, a hydrogen/nitrogen flashlamp (1.8 ns pulse width) was used. The kinetic traces were fitted by monoexponential decay functions using a reconvolution procedure to separate from the lamp pulse profile. Measurements were done in N_2-outgassed *n*-hexane at room temperature (23 °C) in cuvettes of 1 cm path length. For fluorescence quantum yield measurements, the absorbance at the excitation wavelength was kept around 0.2. (*S*)-6-Methoxy-α-methyl-2-naphthaleneacetic acid [(*S*)-naproxen] in acetonitrile was used as the fluorescence standard ($\Phi_f = 0.47$ under nitrogen).[45]

Synthesis of the Dyads and the Model Compounds. The synthesis of the dyads was accomplished by reaction of 0.8 mmol (*S*)-6-methoxy-α-methyl-2-naphthaleneacetic acid [(*S*)-naproxen] with 1 mmol (*S*)- or (*R*)-(1-naphthyl)ethylamine in 10 mL of dry dichloromethane. 1-(3-Dimethylaminopropyl)-*N*-ethylcarbodiimide hydrochloride (EDC, 1.0 mmol) was used for the activation of the acid. After standard workup, the compounds were purified by flash chromatography (ethyl acetate/*n*-hexane, 7:3).

Model compound NPX-M was synthesized by reaction of 0.8 mmol (*S*)-6-methoxy-α-methyl-2-naphthaleneacetic acid with 1.0 mmol diethylamine in the presence of 1.0 mmol EDC in 10 mL of dry dichloromethane. The preparation of NAP-M was accomplished by reacting 0.9 mmol (*R*)-(1-naphthyl)ethylamine with a slight excess of acetyl chloride (1.1 mmol) in the presence of 1.2 mmol triethylamine in 10 mL of dry dichloromethane. After standard workup, the products were purified by flash chromatography (ethyl acetate/*n*-hexane, 7:3). All compounds were subsequently recrystallized from mixtures of *n*-hexane and dichloromethane and characterized by ^{1}H and ^{13}C NMR spectroscopy and elemental analysis.

2(S)-(6-Methoxynaphth-2-yl)-N-[(1(S)-naphth-1-yl)ethyl)]propionamide [(S,S)-NPX-NAP]. ^{1}H NMR (300 MHz, $CDCl_3$) δ (ppm): 1.55 (d, $J = 6.8$ Hz, 3H, CH_3), 1.57 (d, $J = 7.2$ Hz, 3H, CH_3), 3.68 (q, $J = 7.2$ Hz, 1H, CH), 3.88 (s, 3H, CH_3O), 3.68 (s, 1H, NH), 5.84 (q, $J = 6.8$ Hz, 1H, CH), 7.05−7.13 (m, 2H, arom. CH), 7.17−7.43 (m, 5H, arom. CH), 7.51−7.63 (m, 3H, arom. CH), 7.68 (d, $J = 8.1$ Hz, 1H, arom. CH), 7.77 (d, $J = 8.1$ Hz, 1H, arom. CH), 7.91 (d, $J = 8.3$ Hz, 1H, arom. CH). ^{13}C NMR (75 MHz, $CDCl_3$) δ (ppm): 18.5 (CH_3), 20.8 (CH_3), 44.9 (CH), 47.1 (CH), 55.3 (CH_3O), 105.6, 118.9, 122.3, 123.4, 125.0, 125.7, 126.0, 126.2, 126.3, 127.4, 128.1, 128.6 (arom. CH), 128.9 (arom. C), 129.2 (arom. CH), 131.0, 133.7, 133.8, 136.3, 138.3, 157.7 (arom. C), 173.1 (CO). Anal. Calcd for $C_{26}H_{25}NO_2$: C, 81.43; H, 6.57; N, 3.65. Found: C, 81.59; H, 6.60; N, 3.68.

2(S)-(6-Methoxynaphth-2-yl)-N-[(1(R)-naphth-1-yl)ethyl)]propionamide [(S,R)-NPX-NAP]. ^{1}H NMR (300 MHz, $CDCl_3$) δ (ppm): 1.45 (d, $J = 6.4$ Hz, 3H, CH_3), 1.52 (d, $J = 7.0$ Hz, 3H, CH_3), 3.55 (q, $J = 7.0$ Hz, 1H, CH), 3.87 (s, 3H, CH_3O), 5.79 (s, 1H, NH), 5.86 (q, $J = 6.4$ Hz, 1H, CH), 7.07−7.15 (m, 2H, arom. CH), 7.27−7.51 (m, 5H, arom. CH), 7.57 (s, 1H, arom. CH), 7.62 (d, $J = 8.9$ Hz, 1H, arom. CH), 7.67 (d, $J = 8.5$ Hz, 1H, arom. CH), 7.72 (dd, $J = 7.6$ Hz, $J = 1.5$ Hz, 1H, arom. CH), 7.79−7.85 (m, 1H, arom. CH), 8.00−8.07 (m, 1H, arom. CH). ^{13}C NMR (75 MHz, $CDCl_3$) δ (ppm): 18.6 (CH_3), 20.4 (CH_3), 44.8 (CH), 46.9 (CH), 55.3 (CH_3O), 105.7, 119.1, 122.5, 123.4, 125.1, 125.7, 126.0, 126.1, 126.4, 127.4, 128.2, 128.6 (arom. CH), 128.9 (arom. C), 129.2 (arom. CH), 131.0, 133.6, 133.8, 136.5, 138.3, 157.6 (arom. C), 173.0 (CO). Anal. Calcd for $C_{26}H_{25}NO_2$: C, 81.43; H, 6.57; N, 3.65. Found: C, 80.92; H, 6.74; N, 3.73.

N,N-Diethyl-2(S)-(6-methoxynaphth-2-yl)propionamide (NPX-M). ^{1}H NMR (300 MHz, $CDCl_3$) δ (ppm): 0.99 (t, $J = 7.2$ Hz, 3H, N−$CH_2C\mathit{H_3}$), 1.09 (t, $J = 7.2$ Hz, 3H, N−$CH_2C\mathit{H_3}$), 1.50 (d, $J = 6.8$ Hz, 3H, CH_3), 3.10 (dq, $J = 14.0$ Hz, $J = 7.2$ Hz, 1H, N−CH_2), 3.27 (dq, $J = 14.0$ Hz, $J = 7.2$ Hz, 1H, N−CH_2), 3.37 (dq, $J = 14.0$ Hz, $J = 7.2$ Hz, 1H, N−CH_2), 3.54 (dq, $J = 14.0$ Hz, $J = 7.2$ Hz, 1H, N−CH_2), 3.90 (s, 3H, CH_3O), 3.94 (q, $J = 6.8$ Hz, 1H, CH), 7.07−7.15 (m, 2H, arom. CH),

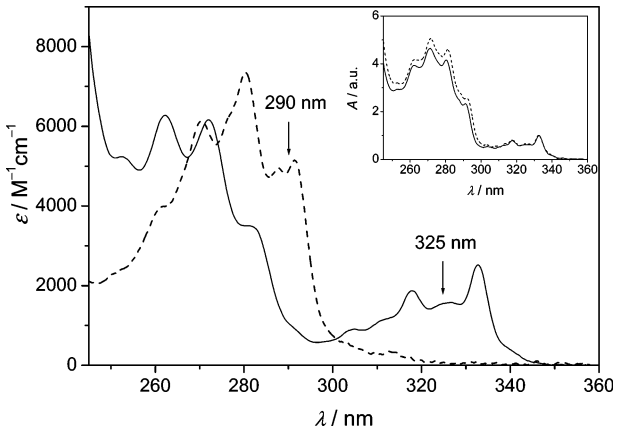

Figure 1. Absorption spectra of the model compounds NPX-M (full line) and NAP-M (dashed line) in *n*-hexane. The arrows indicate the two selected wavelengths for specific excitation of one or the other chromophore. The inset shows the summed up spectra of the model compounds (full line) and the spectrum of (*S*,*S*)-NPX-NAP (dashed line), both normalized to 1 at 333 nm.

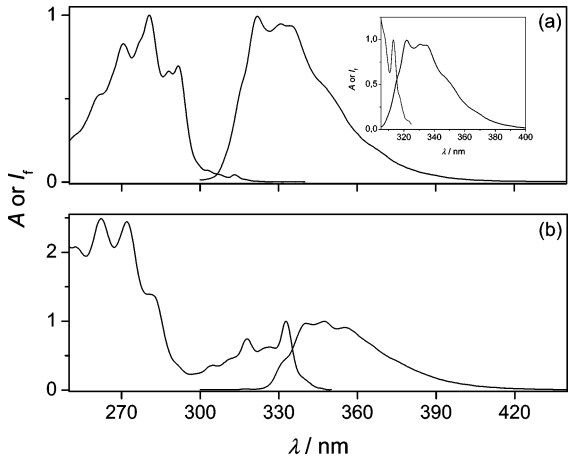

Figure 2. Normalized absorption (left) and fluorescence spectra (right) of (a) NAP-M and (b) NPX-M in *n*-hexane. The fluorescence spectra were obtained with $\lambda_{exc} = 290$ nm. The inset in panel a shows the normalized fluorescence spectrum (left) and the forbidden absorption band at 313 nm (right). From the intersection, the 0−0 excitation energy (E_{0-0}) was extracted.

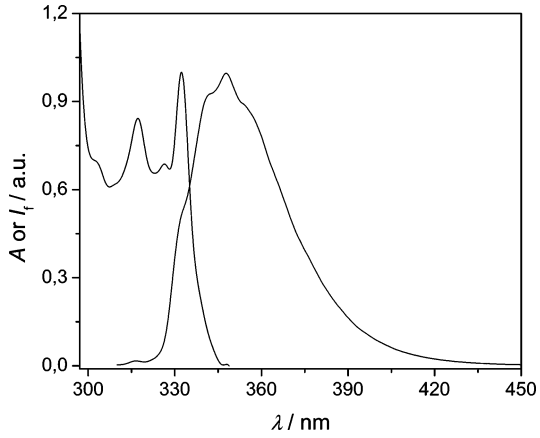

Figure 3. Normalized absorption (left) and fluorescence ($\lambda_{exc} = 290$ nm, right) spectra of (*S*,*R*)-NPX-NAP in *n*-hexane.

7.40 (dd, $J = 8.5$ Hz, $J = 1.9$ Hz, 1H, arom. CH), 7.62 (s, 1H, arom. CH), 7.68 (d, $J = 3.2$ Hz, 1H, arom. CH), 7.70 (d, $J = 3.0$ Hz, 1H, arom. CH). ^{13}C NMR (75 MHz, $CDCl_3$) δ (ppm): 12.9 (N−CH_2CH_3), 14.3 (N−CH_2CH_3), 21.0 (CH_3), 40.3 (N−CH_2), 41.7 (N−CH_2), 43.1 (CH), 55.4 (CH_3O), 105.7, 118.9, 125.5, 126.3, 127.4, 129.2 (arom. CH), 129.3, 133.5, 137.7, 157.6 (arom. C), 172.9 (CO). Anal. Calcd for $C_{18}H_{23}NO_2$: C, 75.76; H, 8.12; N, 4.91. Found: C, 75.57; H, 8.10; N, 4.90.

N-[(1(R)-Naphth-1-yl)ethyl]acetamide (NAP-M). ^{1}H NMR (300 MHz, $CDCl_3$) δ (ppm): 1.67 (d, $J = 6.6$ Hz, 3H, CH_3), 1.97 (s, 3H, $COCH_3$), 5.66 (s, 1H, NH), 5.92 (q, $J = 6.6$ Hz, 1H, CH), 7.42−7.59 (m, 4H, arom. CH), 7.80 (d, $J = 7.7$ Hz, 1H, arom. CH), 7.87 (d, $J = 7.7$ Hz, 1H, arom. CH), 8.10 (d, $J = 8.3$ Hz, 1H, arom. CH). ^{13}C NMR (75 MHz, $CDCl_3$) δ (ppm): 20.7 (CH_3), 23.4 ($COCH_3$), 44.7 (CH), 122.6, 123.5, 125.2, 126.8, 127.7, 128.5, 128.8 (arom. CH), 131.2, 134.0, 138.2 (arom. C), 168.9 (CO). Anal. Calcd for $C_{14}H_{15}NO$: C, 78.84; H, 7.09; N, 6.57. Found: C, 78.35; H, 7.32; N, 6.67.

Results and Discussion

UV/Vis Absorption Properties. The absorption spectra of both model compounds NPX-M and NAP-M in *n*-hexane are shown in Figure 1. Both chromophores display fine-structured absorption bands, typical for naphthalene and derivatives.[45,46] The spectrum of the bichromophoric dyad (*S*,*S*)-NPX-NAP is shown in the inset of Figure 1 and compared to the sum of the spectra of the model compounds. It can be clearly seen that the spectra of the bichromophoric dyads are a superposition of the absorption spectra of the respective model compounds NAP-M and NPX-M. This is indicative of the absence of any ground-state interaction between both chromophores. Furthermore, no significant differences in the spectra of both diastereomeric dyads were noted; i.e., chiral information has significant impact on neither the spectral distribution nor the oscillator strength of the π,π^*-transitions.

A comparison of the spectra of the naphthalene model compounds revealed two favorable wavelengths for the excitation of the NPX-NAP dyads: 290 and 325 nm (arrows in Figure 1). At 325 nm, exclusively NPX was excited, since NAP has no absorption at this wavelength. On the other hand, at 290 nm NAP absorbed the main fraction of photons (compare $\epsilon_{290} = 4884$ and 1058 M^{-1} cm^{-1} for NAP-M and NPX-M, respectively). This enabled us to excite specifically or at least preferentially each of the chromophores. These absorption features have consequences for the wavelength-dependent photophysics of NPX-NAP.

Fluorescence Measurements. The fluorescence spectra obtained upon excitation of the model compounds in *n*-hexane at 290 nm showed typical fine-structured bands, but with different maxima (cf. Figure 2).[45,46] For NAP-M the maximum was found at 321 nm. On the other hand, the fluorescence maximum of NPX-M was shifted to 347 nm.

Strikingly, upon excitation at 290 and 325 nm the fluorescence spectra of the bichromophoric dyads solely displayed an emission band centered at 347 nm (cf. Figure 3). This fluorescence can be unambiguously identified as originating from NPX, based on comparison with the model compounds. The latter observation indicates that when the major part of the excitation energy at $\lambda_{exc} = 290$ nm is absorbed by NAP, an efficient singlet−singlet energy transfer from NAP to NPX must happen in the dyads (see below).

From the intersection between normalized absorption and emission spectra of the dyads NPX-NAP, an excited singlet state energy (E_{0-0}) of 3.70 eV can be extracted for both diastereomers. This value compares favorably with the one determined for the model compound NPX-M (3.70 eV) and the reported value of 3.69 eV for (*S*)-naproxen.[47] The E_{0-0} of the model

TABLE 1: Photophysical Parameters of the Dyads and the Relevant Model Compounds

	Φ_f (λ_{exc} = 290 nm)[a]	Φ_f (λ_{exc} = 325 nm)[a]	τ_f/ns (λ_{exc} = 290 nm)[b]	τ_f/ns (λ_{exc} = 325 nm)[b]
(*S*,*S*)-NPX-NAP	0.34 ± 0.02	0.59 ± 0.03	13.2	13.4
(*S*,*R*)-NPX-NAP	0.34 ± 0.02	0.61 ± 0.02	13.2	13.4
NPX-M[c]	0.35 ± 0.02	0.62 ± 0.02	14.1	14.4
NAP-M[d]	0.18 ± 0.01		52.7	

[a] Fluorescence quantum yield in deaerated acetonitrile, measured with (*S*)-naproxen as the standard; see Experimental Section. [b] Fluorescence lifetime measured at λ_{obs} = 347 nm in deaerated acetonitrile; measured with single-photon-counting; 5% error. [c] (*S*)-enantiomer. [d] (*R*)-enantiomer.

NAP-M, 3.93 eV, is in excellent agreement with the value for 1-methylnaphthalene (3.90 eV).[48] From these data it becomes clear that singlet−singlet energy transfer from NAP to NPX is thermodynamically favored ($\Delta G_{SSET} = -0.23$ eV).

To account for the quantification of radiative processes in the dyads, fluorescence quantum yields and lifetimes were measured for both model compounds and bichromophoric dyads. The data are compiled in Table 1.

The photophysical data for NPX-M and NAP-M are in good agreement with those reported for their respective parent chromophores, e.g., naproxen ($\Phi_f = 0.47$ and $\tau_f = 10.8$ ns; in acetonitrile)[45] and 1-methylnaphthalene ($\Phi_f = 0.26$ and τ_f = 67.0 ns; in cyclohexane).[49] By comparing the fluorescence quantum yields in Table 1, two conclusions can be drawn: (1) the fluorescence quantum yield upon excitation of the dyads at 290 nm is ca. 2 times larger than the quantum yield of the NAP-M model compound and is practically identical with that of NPX-M, indicating an efficient energy transfer, and (2) the fluorescence quantum yields of the dyads and NPX-M are larger for excitation at 325 nm than for 290 nm, pointing to an increased contribution of an additional decay channel at shorter wavelengths.

Energy Transfer in the Dyads. A detailed analysis of the parameters involved in the energy transfer results in the following relations (eqs 1−3), which allow for the extraction of the rate constants of intramolecular singlet−singlet energy transfer (SSET) in the dyads. The fluorescence quantum yield of NPX in the dyads at λ_{exc} = 290 nm breaks up into two contributions: the fluorescence which is sensitized by energy transfer from NAP (first term in eq 1) and the fluorescence which results from direct excitation of NPX (second term in eq 1). The contributions of both pathways are weighted by the relative light absorption of both chromophores at 290 nm. For low optical densities (as applies to our experiments), the molar absorption coefficients can be used to define the respective fractions of absorbed photons. With the help of eq 1, the quantum yield for SSET in both dyads can be calculated. Equation 2 allows for the determination of the NAP lifetime τ_{NAP} in the dyads, and eq 3 defines the rate constant of SSET (k_{SSET}).

$$\Phi_{f,NPX}^{290} = \left(\frac{\epsilon_{NAP\text{-}M}^{290}}{\epsilon_{NAP\text{-}M}^{290} + \epsilon_{NPX\text{-}M}^{290}}\right)\Phi_{SSET}\Phi_{f,NPX\text{-}M}^{290} + \left(\frac{\epsilon_{NPX\text{-}M}^{290}}{\epsilon_{NAP\text{-}M}^{290} + \epsilon_{NPX\text{-}M}^{290}}\right)\Phi_{f,NPX\text{-}M}^{290} \quad (1)$$

with

$$\frac{\epsilon_{NAP\text{-}M}^{290}}{\epsilon_{NAP\text{-}M}^{290} + \epsilon_{NPX\text{-}M}^{290}} = 0.82$$

and

$$\frac{\epsilon_{NPX\text{-}M}^{290}}{\epsilon_{NAP\text{-}M}^{290} + \epsilon_{NPX\text{-}M}^{290}} = 0.18$$

$$\tau_{NAP} = \tau_{NAP\text{-}M}(1 - \Phi_{SSET}) \quad (2)$$

$$k_{SSET} = \frac{1}{\tau_{NAP}} - \frac{1}{\tau_{NAP\text{-}M}} \quad (3)$$

With the known molar absorption coefficients of the model compounds, the lifetime of NAP-M, and the fluorescence quantum yield of NPX-M (λ_{exc} = 290 nm), the following lifetime τ_{NAP} and rate constant k_{SSET} are calculated for the two diastereomeric dyads NPX-NAP: $\tau_{NAP} = 1.8$ ns; $k_{SSET} = (5.3 \pm 0.3) \times 10^8$ s^{-1}. These data are the same for both dyads. According to eq 1, the quantum yield of energy transfer amounts to about 97% (±3%) indicating a high efficiency of the process. Due to the almost quantitative energy transfer, no residual fluorescence of NAP can be seen in the fluorescence spectra of the dyads.

The calculation of the spectral overlap integrals for singlet−singlet energy transfer in our dyads yielded the following values for the application of the Förster ($J_{dipole-dipole}$) or Dexter ($J_{exchange}$) mechanism: $J_{dipole-dipole} = 1.23 \times 10^{-12}$ cm^6 mol^{-1}, $J_{exchange} = 2.07 \times 10^{-4}$ cm.[17] The Förster theory defines a critical distance (R_0), where the energy transfer probability is 50% (eq 4), which was estimated to $R_0 = 16.9$ Å for the investigated dyads NPX-NAP. Molecular modeling (AM1) of the dyads resulted in a center-to-center distance of ca. 6.5 Å between both naphthalene moieties. For such distance, a rate constant of $k_{SSET} = 5.9 \times 10^9$ s^{-1} would be expected, based on dipole−dipole interaction (eq 4). On the other hand, the observed rate constant for the dyads is 1 order of magnitude lower. Thus, based on our observations it cannot be decided clearly whether the Förster or Dexter mechanism prevails. Due to the rather high flexibility of the spacer in the dyads, also extended conformations with larger donor−acceptor distances are expected as local minima. For these situations ($R \geq 10$ Å), clearly Förster energy transfer should be dominant, due to the missing orbital overlap between donor and acceptor, as it is required for Dexter energy transfer. However, for the further discussion (see below) related to the quenching of both naphthalene chromophores by electron-donating amines, the actual energy transfer mechanism has no implications.

$$k_{dipole-dipole} = \frac{1}{\tau_D}\left(\frac{R_0}{R}\right)^6 \quad \text{with } R_0^{\,6} = \frac{9000 \ln 10 \kappa^2 \Phi_D}{128\pi^5 n^4 N_A} J_{dipole-dipole} \quad (4)$$

Quenching of the Model Compounds by Triethylamine. Thermodynamics of Electron Transfer versus Exciplex Formation. Typical photoinduced reactions of naphthalene and its derivatives are electron transfer (et) or exciplex formation (ex) with appropriate electron donors such as amines.[37−44] First, the fluorescence of model compounds NPX-M and NAP-M was quenched by triethylamine (TEA). Since nonpolar *n*-hexane was

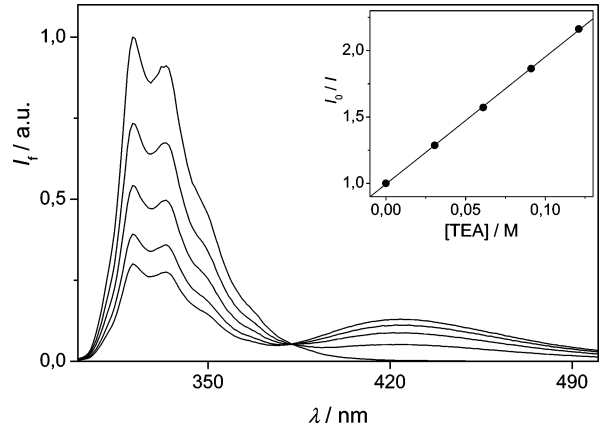

Figure 4. Steady-state fluorescence quenching of NAP-M by triethylamine (TEA) in *n*-hexane. The fluorescence spectra were obtained at $\lambda_{exc} = 290$. The inset shows the corresponding Stern−Volmer plot.

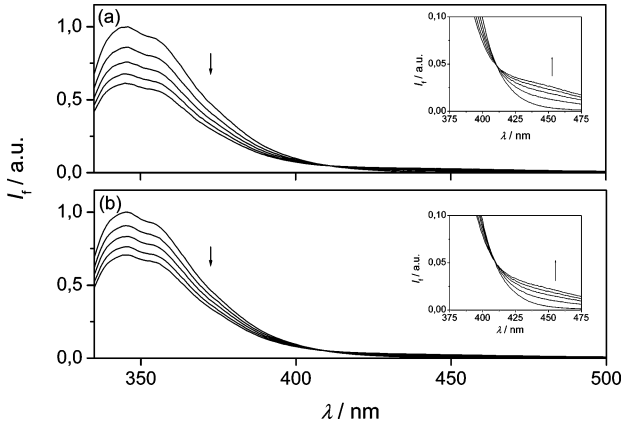

Figure 5. Steady-state fluorescence quenching of (a) (*S*,*S*)-NPX-NAP and (b) (*S*,*R*)-NPX-NAP by TEA in *n*-hexane. The fluorescence spectra were obtained at $\lambda_{exc} = 325$ nm. The insets show the development of the exciplex emission bands.

used as the solvent, exciplex formation should dominate over photoinduced electron transfer. For the calculation of the free energy for the formation of the radical ion pair (ΔG_{et}) in *n*-hexane, eq 5 was used.[50]

$$\Delta G_{et} = E_{ox} - E_{red} - E_{0-0} + \frac{2.6\ \text{eV}}{\epsilon} - 0.13\ \text{eV} \qquad (5)$$

With this equation, the free energy associated with radical ion pair formation upon photoinduced electron transfer from triethylamine can be calculated as $\Delta G_{et} = 1.02$ and 0.77 eV for NPX-M and NAP-M, respectively.[51] Thus, this quenching pathway is characterized by strongly endergonic thermodynamics and is highly unlikely. For the free energy of exciplex formation ΔG_{ex}, eq 6 applies.[50]

$$\Delta G_{ex} = E_{ox} - E_{red} - E_{0-0} - \frac{\mu^2}{\rho^3}\left(\frac{\epsilon - 1}{2\epsilon + 1} - 0.19\right) + 0.38\ \text{eV} \qquad (6)$$

Using the same electrochemical potentials and excited singlet state energies as in eq 5[51] and an average value of 0.75 eV for μ^2/ρ^3,[50] ΔG_{ex} is equal to 0.16 and −0.09 eV for NPX-M and NAP-M, respectively. Strikingly, these estimations are excellently verified by the experimental observations. Indeed, for NAP-M the quenching is accompanied by a broad and red-shifted emission band at ca. 435 nm (cf. Figure 4), typical for a naphthalene-amine exciplex as reported for several related systems.[37,39,40,52] On the other hand, no quenching was observed for NPX-M as predicted by the endergonic thermodynamics for exciplex formation.

The bimolecular quenching rate constant of NAP-M by triethylamine was obtained in two ways: (i) from the Stern−Volmer plot shown in the inset of Figure 4 and (ii) by measuring the NAP-M fluorescence lifetimes in the presence of increasing TEA concentrations. The two values were practically identical [$(6.5 \pm 0.3) \times 10^9$ M^{-1} s^{-1}]. This quenching rate constant is 1 order of magnitude below diffusion control and accounts very well for the estimated exergonicity of exciplex formation.

To verify our observations, a control experiment was performed, using 1,4-diazabicyclo[2.2.2]octane (DABCO) as a stronger electron-donating amine [$E_{ox} = 0.68$ V versus 0.88 V for triethylamine (saturated calomel electrode (SCE), acetonitrile)].[53] Now for both model compounds NAP-M and NPX-M an exergonic thermodynamics for exciplex formation is expected.[54] And indeed, dynamic quenching accompanied by high rate constants was observed in both cases [$(8.1 \pm 0.4) \times 10^9$ M^{-1} s^{-1} for NAP-M and $(4.7 \pm 0.2) \times 10^9$ M^{-1} s^{-1} for NPX-M].

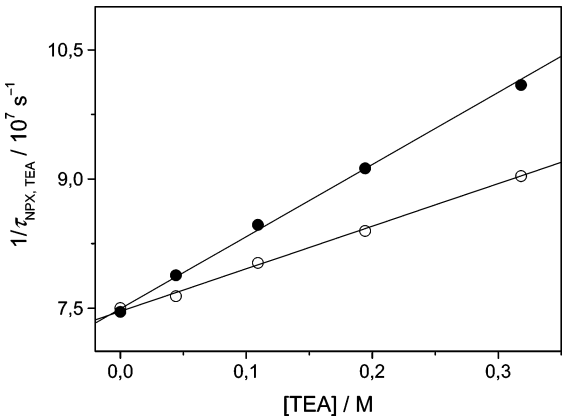

Figure 6. Plots of the inverse lifetime of NPX versus TEA concentration. The data were obtained from time-resolved fluorescence quenching of (*S*,*S*)-NPX-NAP (full circles) and (*S*,*R*)-NPX-NAP (open circles) by TEA at $\lambda_{exc} = 325$ nm in *n*-hexane.

Fluorescence Quenching of NPX-NAP Dyads by Triethylamine at $\lambda_{exc} = 325$ nm. Excitation of the dyads at 325 nm leads exclusively to excited states of NPX. Contrary to the observations made for the model compound NPX-M (see above), the fluorescence of the NPX-chromophore in both dyads is quenched by triethylamine in a dynamic process. The bimolecular quenching rate constants can be simply determined by application of the Stern−Volmer equation: $I_0/I = \tau_0/\tau = 1 + k_q\tau_0$[TEA]. Bimolecular quenching rate constants obtained from steady-state fluorescence measurements were $(1.1 \pm 0.1) \times 10^8$ M^{-1} s^{-1} and $(7.4 \pm 0.4) \times 10^7$ M^{-1} s^{-1} for (*S*,*S*)- and (*S*,*R*)-NPX-NAP, respectively (cf. Figure 5). The values derived from time-resolved measurements were somewhat smaller [$(8.5 \pm 0.4) \times 10^7$ M^{-1} s^{-1} and $(4.9 \pm 0.2) \times 10^7$ M^{-1} s^{-1} for (*S*,*S*)- and (*S*,*R*)-NPX-NAP, respectively, cf. Figure 6], presumably due to a small contribution of static quenching in the steady-state experiments.

Evidently, exciplexes are involved in the quenching mechanism of NPX in the dyads, as can be seen by the typical broad and red-shifted emission band (cf. insets in Figure 5). Interestingly, the diastereomeric dyads show significant stereodifferentiation in the reactivity toward electron-donating triethylamine. The rate constants differ by a factor of 1.7.

CHART 2

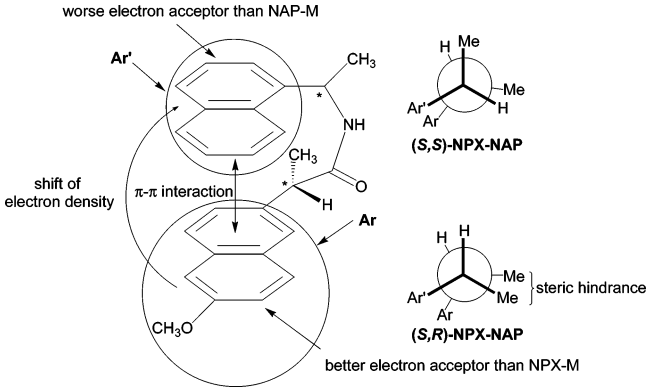

The different behavior of the NPX-chromophore in the model compound NPX-M and in the dyads (NPX-NAP) implies that the reduction potential of NPX is increased in the NPX-NAP. On the other hand, a change of the excited state energy of NPX cannot be deemed responsible, as clearly can be seen from the matching absorption spectra of model compounds and dyads (cf. inset in Figure 1). The increased NPX reduction potential in the dyads can be explained by a $\pi-\pi$ interaction of both chromophores, which shifts electron density from NPX to NAP. Therefore, NPX acts as a better electron acceptor in the dyads (cf. Chart 2).

To achieve a favorable interaction between the π-systems of both chromophores, the spacer has to attain a certain conformation, whose stability might be strongly dependent on the configuration of both chiral centers. Obviously, this is facilitated when both asymmetric carbons are in their *S* configuration, as indicated by the higher quenching rate constant of NPX in the (*S*,*S*) dyad.

Fluorescence Quenching of NPX-NAP Dyads by Triethylamine at $\lambda_{exc} = 290$ nm. Quenching experiments of dyad fluorescence by triethylamine were also performed at $\lambda_{exc} = 290$ nm, where light is preferentially absorbed by NAP. The high quenching rate constant of the model compound NAP-M by triethylamine [$k_q = (6.5 \pm 0.3) \times 10^9$ M^{-1} s^{-1}] suggests that exciplex formation with excited NAP in the dyads can compete with singlet−singlet energy transfer to NPX (see above) already at amine concentrations of ca. 0.1 M. As for the model compound NAP-M, exciplex emission at ca. 435 nm was observed with increasing fluorescence quenching of the dyads at $\lambda_{exc} = 290$ nm (cf. Figure 7).

The determination of the bimolecular rate constant of NAP quenching in the dyads by triethylamine is based on eqs 7 and 8.

$$\Phi^{290}_{f,NPX,TEA} = \left(\frac{\epsilon^{290}_{NAP\text{-}M}}{\epsilon^{290}_{NAP\text{-}M} + \epsilon^{290}_{NPX\text{-}M}}\right)\tau_{NAP,TEA}k_{SSET}\tau_{NPX,TEA}k^{290}_{f,NPX\text{-}M} + \left(\frac{\epsilon^{290}_{NPX\text{-}M}}{\epsilon^{290}_{NAP\text{-}M} + \epsilon^{290}_{NPX\text{-}M}}\right)\tau_{NPX,TEA}k^{290}_{f,NPX\text{-}M} \quad (7)$$

$$\frac{1}{\tau_{NAP,TEA}} = \frac{1}{\tau_{NAP}} + k_{q,NAP}[TEA] \quad (8)$$

Equation 7 describes, similar to eq 1, the two contributions to the fluorescence of NPX in the dyads at each triethylamine concentration at $\lambda_{exc} = 290$ nm, i.e., sensitization by SSET and direct excitation. The rate constant for radiative decay of NPX

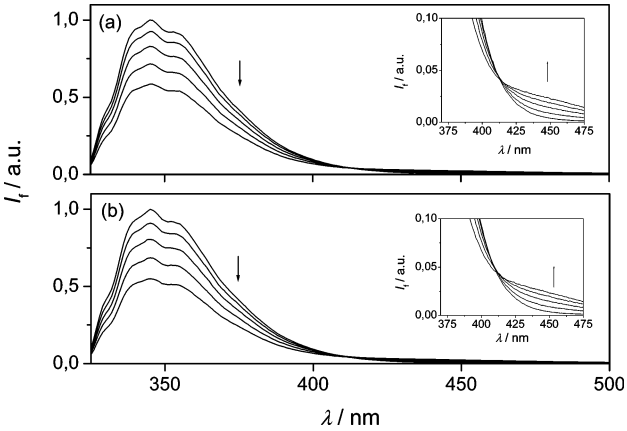

Figure 7. Steady-state fluorescence quenching of (a) (*S*,*S*)-NPX-NAP and (b) (*S*,*R*)-NPX-NAP by TEA in *n*-hexane. The fluorescence spectra were obtained at $\lambda_{exc} = 290$ nm. The insets show the development of the exciplex emission bands.

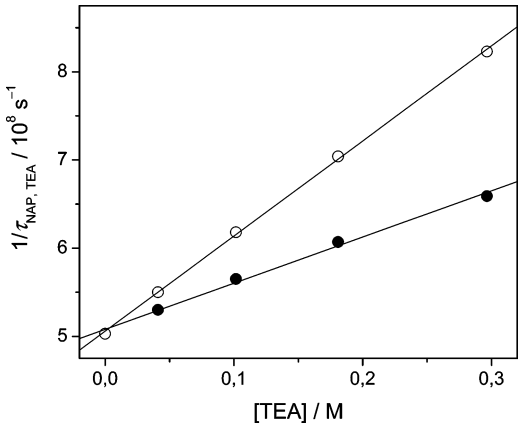

Figure 8. Plots of the inverse lifetime of NAP versus TEA concentration according to eq 8. The data were obtained from fluorescence quenching of (*S*,*S*)-NPX-NAP (full circles) and (*S*,*R*)-NPX-NAP (open circles) by TEA at $\lambda_{exc} = 290$ nm in *n*-hexane.

was calculated with $k^{290}_{f,NPX\text{-}M} = \Phi^{290}_{f,NPX\text{-}M}/\tau^{290}_{NPX\text{-}M}$. Furthermore, the lifetime of NPX in the dyads at each triethylamine concentration ($\tau_{NPX,TEA}$) is known by time-resolved fluorescence quenching of NPX-NAP at $\lambda_{exc} = 325$ nm. Based on eq 7 the lifetime of the NAP chromophore ($\tau_{NAP,TEA}$) at each triethylamine concentration was calculated and then plotted according to eq 8 (cf. Figure 8). The slope of a plot according to eq 8 yields the bimolecular rate constant for quenching by exciplex formation between triethylamine and NAP for each dyad: $k_{q,NAP} = (5.3 \pm 0.3) \times 10^8$ M^{-1} s^{-1} and $(1.1 \pm 0.1) \times 10^9$ M^{-1} s^{-1} for (*S*,*S*)-NPX-NAP and (*S*,*R*)-NPX-NAP, respectively. From the intercept, the lifetime of NAP without added quencher can be calculated: $\tau_{NAP} = 2.0$ ns. This lifetime is in excellent agreement with the one derived from the treatment of the SSET process in the dyads (see above).

Similar to the quenching of NPX at $\lambda_{exc} = 325$ nm, a significant stereodifferentiation in the reactivity of NAP was observed for both diastereomeric dyads. But now, the (*S*,*R*)-diastereomer reacts faster by a factor of 2.1, while for NPX quenching (*S*,*S*)-NPX-NAP is more reactive toward triethylamine. Conclusively, there is an inversion of diastereodifferentiation upon going from NPX to NAP.

The observed inverted behavior of NAP compared with NPX in the dyads is not unexpected, following our explanation of a changed reduction potential of the chromophores in the dyads, mediated by configuration-dependent $\pi-\pi$ interactions. If, as

shown above (cf. Chart 2), NPX is a better electron acceptor in the (*S*,*S*) dyad, NAP must be a worse acceptor in this diastereomer compared with the (*S*,*R*) combination. Therefore, the diastereodifferentiation for NAP is opposite to that for NPX. Generally, NAP is a worse electron acceptor in the dyads compared with the model NAP-M, as documented by the smaller quenching rate constants in the dyads ($0.5-1.1 \times 10^9$ M^{-1} s^{-1} versus 6.5×10^9 M^{-1} s^{-1}).

Conclusions

In essence, we have demonstrated wavelength-dependent stereodifferentiation in the photophysical processes of novel bichromophoric and diastereomeric naphthalene dyads. While upon excitation at 325 nm the light energy remains in the naproxen-derived moiety (NPX), at 290 nm efficient singlet−singlet energy transfer (Φ_{SSET} of about 97%) from the naphthalene-derived chromophore NAP to NPX dominates. Intermolecular quenching experiments of dyad fluorescence by triethylamine as the electron donor have been performed. The role of exciplexes in the quenching mechanism has been established. For this process a pronounced diastereodifferentiation has been observed. Based on thermodynamic considerations and the presence of typical exciplex emission, we were able to conclude on the alteration of the electron acceptor properties of the naphthalene derivatives in the dyads. This effect is dependent on the electronic interaction and, therefore, on the configuration-dependent interaction between both chromophores.

Acknowledgment. The authors thank the Generalitat Valenciana (Grupos 03/082) and the MCYT (Grant BQU 2001-2725 and doctoral fellowship to S.A.) for financial support. The Deutsche Forschungsgemeinschaft (DFG) and the Universidad Politécnica de Valencia are gratefully acknowledged for research fellowships for U.P.

Supporting Information Available: A table with fluorescence quantum yields and lifetimes of dyads and model compounds in aerated *n*-hexane, a table with quenching data of dyads and model compounds by triethylamine in aerated *n*-hexane, ^1H and ^{13}C NMR spectra of dyads and model compounds, and AM1 optimized folded conformers of the dyads. This material is available free of charge via the Internet at http://pubs.acs.org.

References and Notes

(1) Turro, N. J.; Ramamurthy, V.; Cherry, W.; Farneth, W. *Chem. Rev.* **1978**, *78*, 125−145.
(2) Dauben, W. G.; Cogen, J. M.; Behar, V.; Schultz, A. G.; Geiss, W.; Taveras, A. G. *Tetrahedron Lett.* **1992**, *33*, 1713−1716.
(3) Dauben, W. G.; Hecht, S. *J. Org. Chem.* **1998**, *63*, 6102−6107.
(4) Bochet, C. G. *Angew. Chem., Int. Ed.* **2001**, *40*, 2071−2073.
(5) Blanc, A.; Bochet, C. G. *J. Org. Chem.* **2002**, *67*, 5567−5577.
(6) Jacobs, H. J. C.; Havinga, E. *Adv. Photochem.* **1979**, *11*, 305−373.
(7) Mazzucato, U.; Momicchioli, F. *Chem. Rev.* **1991**, *91*, 1679−1719.
(8) Saltiel, J.; Zhang, Y.; Sears, D. F., Jr. *J. Am. Chem. Soc.* **1997**, *119*, 11202−11210.
(9) Becker, R. S.; Pelliccioli, A. P.; Romani, A.; Favaro, G. *J. Am. Chem. Soc.* **1999**, *121*, 2104−2109.
(10) Saltiel, J.; Cires, L.; Turek, A. M. *J. Am. Chem. Soc.* **2003**, *125*, 2866−2867.
(11) Inoue, Y. *Chem. Rev.* **1992**, *92*, 741−770.
(12) Inoue, Y.; Wada, T.; Asaoka, S.; Sato, H.; Pete, J.-P. *J. Chem. Soc., Chem. Commun*. **2000**, 251−259.
(13) Saltiel, J.; Choi, J.-O.; Sears, D. F., Jr.; Eaker, D. W.; O'Shea, K. E.; Garcia, I. *J. Am. Chem. Soc.* **1996**, *118*, 7478−7485.
(14) Kavarnos, G. J.; Turro, N. J. *Chem. Rev.* **1986**, *86*, 401−449.
(15) Scaiano, J. C. *J. Photochem.* **1973**, *2*, 81−118.
(16) Nau, W. M. *Ber. Bunsen-Ges. Phys. Chem.* **1998**, *102*, 476−485.
(17) Speiser, S. *Chem. Rev.* **1996**, *96*, 1953−1976.
(18) Jacques, P.; Allonas, X.; Suppan, P.; von Raumer, M. *J. Photochem. Photobiol., A* **1996**, *101*, 183−184.
(19) von Raumer, M.; Suppan, P.; Haselbach, E. *Helv. Chim. Acta* **1997**, *80*, 719−724.
(20) Pischel, U.; Zhang, X.; Hellrung, B.; Haselbach, E.; Muller, P.-A.; Nau, W. M. *J. Am. Chem. Soc.* **2000**, *122*, 2027−2034.
(21) Pischel, U.; Nau, W. M. *J. Am. Chem. Soc.* **2001**, *123*, 9727−9737.
(22) Griller, D.; Howard, J. A.; Marriott, P. R.; Scaiano, J. C. *J. Am. Chem. Soc.* **1981**, *103*, 619−623.
(23) Malatesta, V.; Scaiano, J. C. *J. Org. Chem.* **1982**, *47*, 1455−1459.
(24) Nau, W. M.; Cozens, F. L.; Scaiano, J. C. *J. Am. Chem. Soc.* **1996**, *118*, 2275−2282.
(25) Wagner, P. J.; Truman, R. J.; Puchalski, A. E.; Wake, R. *J. Am. Chem. Soc.* **1986**, *108*, 7727−7738.
(26) Burget, D.; Jacques, P.; Vauthey, E.; Suppan, P.; Haselbach, E. *J. Chem. Soc., Faraday Trans.* **1994**, *90*, 2481−2487.
(27) Pischel, U.; Nau, W. M. *J. Phys. Org. Chem.* **2000**, *13*, 640−647.
(28) Coenjarts, C.; Scaiano, J. C. *J. Am. Chem. Soc.* **2000**, *122*, 3635−3641.
(29) Miranda, M. A.; Lahoz, A.; Martínez-Mánez, R.; Boscá, F.; Castell, J. V.; Pérez-Prieto, J. *J. Am. Chem. Soc.* **1999**, *121*, 11569−11570.
(30) Miranda, M. A.; Lahoz, A.; Boscá, F.; Metni, M. R.; Abdelouahab, F. B.; Castell, J. V.; Pérez-Prieto, J. *J. Chem. Soc., Chem. Commun.* **2000**, 2257−2258.
(31) Miranda, M. A.; Martínez, L. A.; Samadi, A.; Boscá, F.; Morera, I. M. *J. Chem. Soc., Chem. Commun.* **2002**, 280−281.
(32) Pischel, U.; Abad, S.; Domingo, L. R.; Boscá, F.; Miranda, M. A. *Angew. Chem., Int. Ed.* **2003**, *42*, 2531−2534.
(33) Pischel, U.; Abad, S.; Miranda, M. A. *J. Chem. Soc., Chem. Commun.* **2003**, 1088−1089.
(34) Boscá, F.; Andreu, I.; Morera, I. M.; Samadi, A.; Miranda, M. A. *J. Chem. Soc., Chem. Commun.* **2003**, 1592−1593.
(35) Jiménez, M. C.; Stiriba, S.-E.; Tormos, R.; Pérez-Prieto, J.; Miranda, M. A. *Photochem. Photobiol. Sci.* **2004**, *3*, 36−38.
(36) Pérez-Prieto, J.; Lahoz, A.; Boscá, F.; Martínez-Mánez, R.; Miranda, M. A. *J. Org. Chem.* **2004**, *69*, 374−381.
(37) Ibemesi, J. A.; El-Bayoumi, M. A.; Kinsinger, J. B. *Chem. Phys. Lett.* **1978**, *53*, 270−272.
(38) Irie, M.; Yorozu, T.; Hayashi, K. *J. Am. Chem. Soc.* **1978**, *100*, 2236−2237.
(39) Van, S.-P.; Hammond, G. S. *J. Am. Chem. Soc.* **1978**, *100*, 3895−3902.
(40) Meeus, F.; Van der Auweraer, M.; De Schryver, F. C. *J. Am. Chem. Soc.* **1980**, *102*, 4017−4024.
(41) Yorozu, T.; Hayashi, K.; Irie, M. *J. Am. Chem. Soc.* **1981**, *103*, 5480−5484.
(42) Avnir, D.; Wellner, E.; Ottolenghi, M. *J. Am. Chem. Soc.* **1989**, *111*, 2001−2003.
(43) Sakurai, T.; Miyoshi, K.; Obitsu, M.; Inoue, H. *Ber. Bunsen-Ges. Phys. Chem.* **1996**, *100*, 46−54.
(44) Pina, F.; Lima, J. C.; Lodeiro, C.; Seixas de Melo, J.; Díaz, P.; Albelda, M. T.; García-España, E. *J. Phys. Chem. A* **2002**, *106*, 8207−8212.
(45) Boscá, F.; Marin, M. L.; Miranda, M. A. *Photochem. Photobiol.* **2001**, *74*, 637−655.
(46) Becker, H. G. O. *Einführung in die Photochemie*; Deutscher Verlag der Wissenschaften: Berlin, 1991.
(47) Martinez, L. J.; Scaiano, J. C. *Photochem. Photobiol.* **1998**, *68*, 646−651.
(48) Murov, S. L.; Carmichael, I.; Hug, G. L. *Handbook of Photochemistry*, 2nd ed.; Marcel Dekker: New York, 1993.
(49) Lentz, P.; Blume, H.; Schulte-Frohlinde, D. *Ber. Bunsen-Ges. Phys. Chem.* **1970**, *74*, 484−488.
(50) Weller, A. *Z. Phys. Chem. Neue Folge* **1982**, *133*, 93−98.
(51) For the calculation of the energetics of radical ion pair or exciplex formation with eqs 5 and 6, we used the following electrochemical potentials (versus SCE and in acetonitrile or dimethylformamide): E_{ox} (TEA) = 0.88 V (cf. ref 53), E_{red} (2-methoxynaphthalene) = −2.60 V, and E_{red} (1-methylnaphthalene) = −2.58 V (cf. ref 48). As excitation energies, the values for the respective model compounds NPX-M and NAP-M were used: E_{0-0} = 3.70 eV (NPX-M) and 3.93 eV (NAP-M); this work. The dielectricity constant ϵ for *n*-hexane was taken as 1.9 (cf.: Reichardt, C. *Solvents and solvent effects in organic chemistry*, 2nd ed.; VCH: Weinheim, 1990).
(52) Chandross, E. A.; Thomas, H. T. *Chem. Phys. Lett.* **1971**, *9*, 393−396.
(53) Jacques, P.; Burget, D.; Allonas, X. *New J. Chem.* **1996**, *20*, 933−937.
(54) Noteworthy, although exciplex-induced quenching by DABCO is possible for both model compounds (ΔG_{ex} = −0.06 and −0.29 eV for NPX-M and NAP-M, respectively), electron transfer is still endergonic in both cases: ΔG_{et} = 0.82 and 0.57 eV for NPX-M and NAP-M, respectively.